Characteristics Of The Saharan Dust Events Observed in The Month of July, 2012 At Miami Florida: Aerosol Physical Characteristics And Vertical Distribution

JERAL ESTUPINAN

National Weather Service, Miami, Florida

DAN GREGORIA

National Weather Service, Miami, Florida

KENNETH J. VOSS

Department of Physics, University of Miami, Florida

ROBERTO ARIAS

University of Puerto Rico at Mayagüez

ABSTRACT

Every year dust sweeps across the Atlantic ocean along the trade winds, and slips into the skies above Florida, and many Caribbean nations. Already this year, there have been numerous instances of this dust in South Florida, providing an opportunity to study the characteristics of these events in more detail. This study compares surface observations of Aerosol Optical Depth (AOD) from the AERONET (AErosol RObotic NETwork) and a micropulse LIDAR with polarization from the University of Miami South Florida's Cloud-Aerosol-Rain Observatory (CAROb) for several Saharan dust events observed in Miami Florida during the summer season of 2012. The surface observations are then compared with aerosol predictions results from the Navy Aerosol Analysis and Prediction System (NAAPS), and the newly appointed GFS model from the National Oceanic and Atmospheric Administration (NOAA) and the National Weather Service (NWS). Details about the vertical extent and evolution of the Saharan dust inside and above the boundary layer are presented for each event. Preliminary comparisons indicate that the Navy aerosol model captured well the observed values of AOD obtained by the AERONET data for the events observed this summer. MODIS/GOES Hybrid images are used to show the geographical coverage of the Saharan dust.

1. Introduction

Africa’s Saharan Desert is the largest source of mineral dust in the world, covering more than 3 million square milles and causing dust particles to blanket African skies. The Saharan Air Layer (SAL) is described as the mostly dry, warm, and occasionally dust-laden layer in the atmosphere that overlies the Atlantic Ocean air, which is regularly cooler and humid. However, as found by Huang et al. (2010) not all dust outbreaks were categorized as dry air outbreaks, with only 23% of dry air outbreaks categorized as dust outbreaks.

As the name suggests, winds blow dust from Saharan storms over to the Atlantic, resulting in SAL. SAL travels on average at a speed of 1000 km/day, taking a full week to travel from the west coast of Africa to the Caribbean Sea and Florida (Huang et al. 2010). The SAL interacts with other weather phenomena, such as thunderstorms, in several ways. ”Dust affects the size of a thunderstorm's anvil, the strength and number of warm updrafts, and the amount of rain that builds up and falls from the heat generated or convective thunderstorms.” “Florida residents not only see more updrafts developing during dust events, but the dust affects the amount of rainfall that reaches the ground, possibly decreasing the precipitation produced by thunderstorms” (Susan et al. 2009). Dust is an aerosol, and aerosols or little particles serve as the center or nuclei (called cloud condensation nuclei) for cloud droplets to form around. These cloud droplets then combine to form raindrops which fall to the ground.”

The amount of SAL affects the amount of sunlight reaching the ground, thus having effect on the long-term weather conditions in the area. According to Chun Zhao (2011) dust particles in the air partially block sunlight and absorb heat during the day. At nightime, the heat radiates from the sky to the land below and warms the surface, making conditions ideal for nocturnal precipitation.

Lau and Kim (2007) found a link between dust and sea surface temperatures. Results showed that the sunlight-blocking effect of Saharan dust caused a cooling of the North Atlantic of 0.37 to 0.72 degrees Fahrenheit between June 2005 and 2006, approximately one-third of the total sea surface cooling in the North Atlantic.

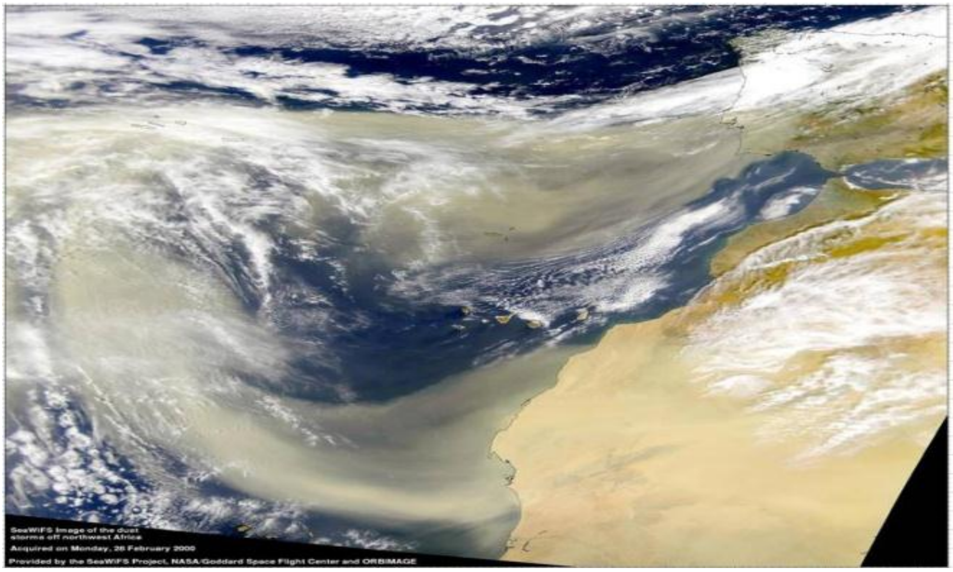

Figure 1. SeaWiFS Image of Dust Storms off Northwest Africa (Provided by the SeaWiFS Project, NASA/Goddard Space Flight Center and ORBIMAGE)

Several Saharan dust events during the month of July of 2012 provided the opportunity to be able to quantify the amount and gain a better understanding of the characteristics of Saharan aerosols that reached South Florida. This was accomplished by comparing surface observations of Aerosol Optical Depth (AOD) from the AERONET (AErosol RObotic NETwork) and a micropulse LIDAR with polarization from the University of Miami South Florida's Cloud-Aerosol-Rain Observatory (CARОb) for the different Saharan dust events observed in Miami Florida during the month of July of 2012. The surface observations are then compared with aerosol predictions results from the Navy Aerosol Analysis and Prediction System (NAAPS), and the new GFS model from the National Oceanic and Atmospheric Administration (NOAA) and the National Weather Service (NWS). Details about the vertical extent and evolution of the Saharan dust are presented for several of the events.

2. Data Sources

a. NRL NAAPS

The Naval Research Laboratory's (NRL) Navy Aerosol Analysis and Prediction System (NAAPS) (Naval Research Laboratory 2012), is a global multi-component aerosol analysis and modeling capability, which combines current and expected satellite data streams with other data that is available and the global aerosol simulation and prediction. Prior to NAAPS, there were no operational analyses of aerosols or operational global capabilities. To make this system more effective, the satellite retrievals are studied, and only the ones that are relevant and practical are implemented. This system is considered one of the most complete suites of aerosol retrieval products in the world.

Among the aerosol optical depth (AOD) products delivered by the NAAPS are: the Total Optical Depth of Sulfate, Dust, and Smoke, Sulfate Surface Concentration, Dust Surface Concentration, and Smoke Surface Concentration.

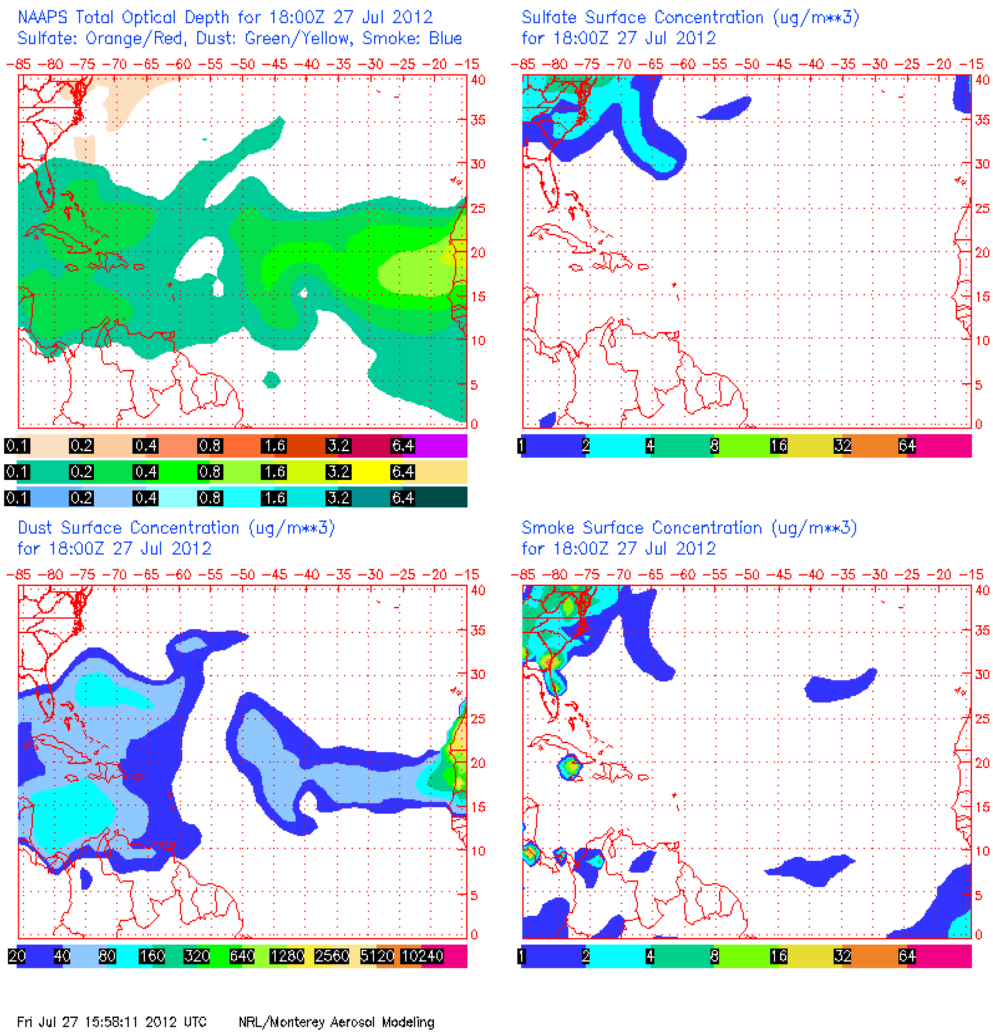

Figure 2. Screen capture of NAAPS products.

b. AERONET

"The AERONET (AErosol RObotic NETwork) program is a federation of ground-based remote sensing aerosol networks established by NASA and PHOTONS (Univ. of Lille 1, CNES, and CNRS-INSU) and is greatly expanded by collaborators from national agencies, institutes, universities, individual scientists, and partners. The program provides a long-term, continuous and readily accessible public domain database of aerosol optical, microphysical and radiative properties for aerosol research and characterization, validation of satellite retrievals, and synergism with other databases. The network imposes standardization of instruments, calibration, processing, and distribution.” (Goddard Space Flight Center 2012)

c. Lidar

Part of the Rosenstiel School of Marine & Atmospheric Science, at the University of Miami “a Sigma micro pulse lidar (MPL, model MPL-4B-IDS-532 with polarization control), is situated inside the penthouse lab, transmitting at 532 nm. The lidar is used for the continuous monitoring of aerosol profiles nominally up to the tropopause. The transmitted beam alternates between co-polarized and cross-polarized states, with the polarization measurements allowing determination of phase for mixed-phase clouds and easing discrimination of aerosol from cloud. The lidar has been running with polarization since December 20, 2011. It has a 1-minute time resolution and a 75 m vertical resolution. The same lidar is used within MPLNET without the polarization.” (Voss 2012).

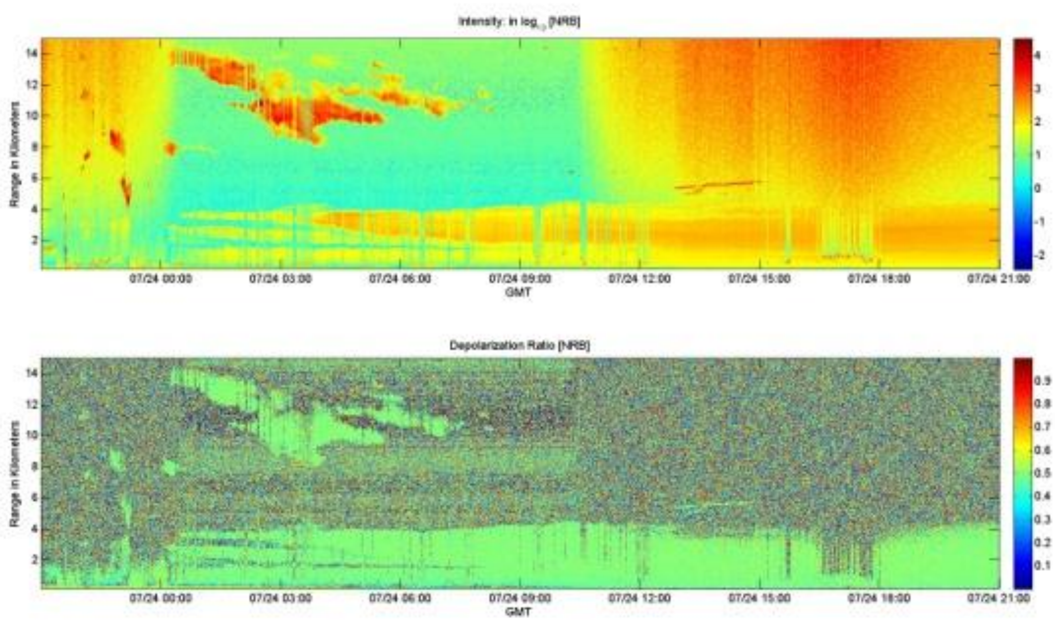

Figure 3. A screen capture of a product by the Lidar. In this case it shows the start of the Saharan dust on 7/24/12.

d. NEMS GFS

The NOAA Environmental Modeling System (NEMS) Global Forecast System (GFS) produces many results for the NOAA NWS, among them forecast lightning maps, and it is now producing SAL forecast maps.

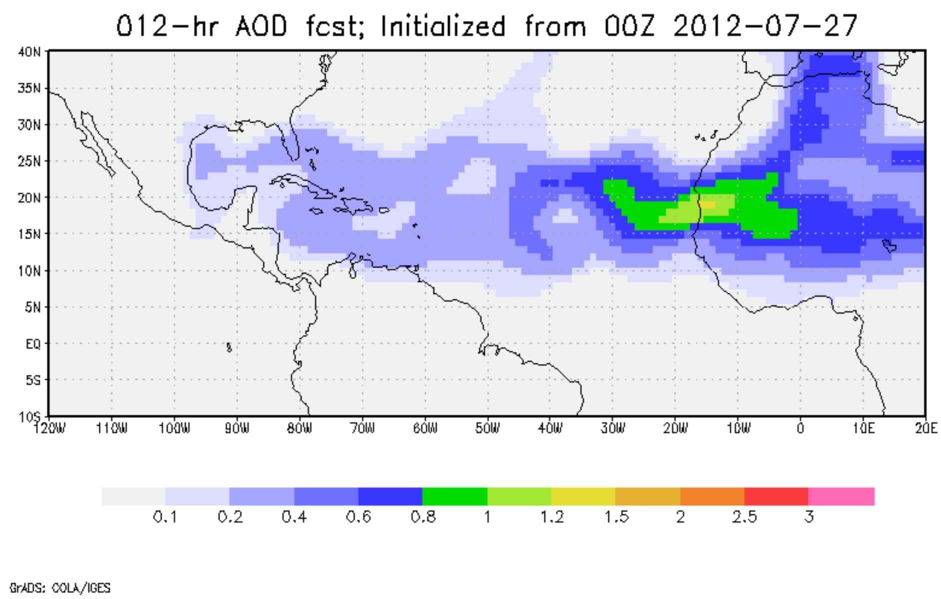

Figure 4. Screen capture of the SAL Evaluation product by the NEMS GFS

3. Results

Six distint Saharan dust events affected the Miami area during the month of July of 2012. Figure 5 shows the average daily AOD from AERONET for the entire month of July. The red circles indicate the days with peak AOD for each of the events. Table 1 lists the length of time where Saharan dust was discernable from a human trained observer. Observations indicate that an AOD greater than 0.15-0.20 can easily be detected by trained human observers as a whitish or mily appearance of the sky and a witish aureole around the sun. A decrease in horizontal visibility is not always required to detect Saharan dust since the dust not always mixes down completely to the surface. An AOD of 0.1 or less is considered to be normal background conditions for Miami corresponding to blue skies and excellent visibility.

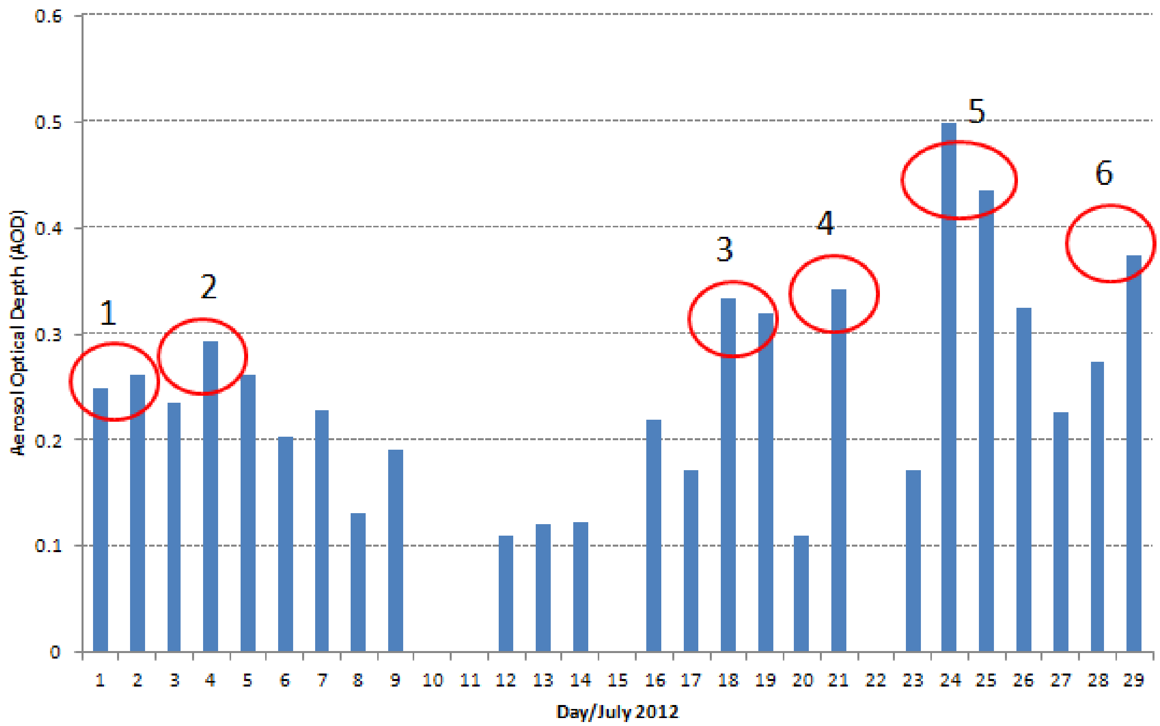

Figure 5. Average daily AOD for the entire month of July of 2012 measured from the AERONET network from Bay Biscayne, south of downtown Miami.

The aerosol optical depth (AOD) is defined as the optical depth due to extinction by the aerosol component of the atmosphere. Aerosol optical depths typically decrease with increasing wavelength and are much smaller for longwave radiation than for shortwave radiation. Values vary widely depending on atmospheric conditions.

The average daily AOD for days with Saharan dust was 0.333 with a maximum of 0.499 and a minimum of 0.262. The average daily AOD for days with no noticeable Saharan dust was 0.182 with a minimum of 0.11 and a maximum of 0.293.

Table 1. Description of the Saharan dust events.

Event Number	Saharan Dust Event	Event Duration	Sounding Characteristics below 5 km
1	Dust was observed between the 2nd and 3rd of July. The 2nd of July exhibited the most dust with a visual decrease in dust observed on the 3rd.	2 days	July 2nd – dry layer 700-800 mb July 3rd – dry layer 800-850 mb Note: For July4th the dry layer was only visible at 750 mb in the morning and it dissipaped in the course of the day.
2	Dust was observed the 5th of	3 days	Not clearly defined drying associated

	July lasting until the morning of the 7^{th}.		with the dust.
3	Dust was observed on the 18^{th} and it was visible until the morning hours of the 20^{th}.	3 days	Strong subsidence inversion first seen at 12z July 18^{th}.
4	Dust was observed on the 21^{st} lasting until the morning of the 22^{nd} when rain and a change in air mass eroded the dust.	1.5 days	Clearly defined dry layer between 650 and 850 mb. A moist sounding is seen at 12z July 22^{nd}.
5	Dust was observed on the 24^{th} lasting into the 26^{th}. However, small amounts of dust persisted into the 28^{th}.	3 days (most noticeable) 5 days total	Clearly defined dry layers. 12z July 24^{th} – 600-850 mb 0z July 25^{th} – 600-900 mb 12z July 25^{th} – 600-900 mb Note: Moistening from below seen at the end.
6	A reinforecement of dust is observed on 7/29 lasting into the 30^{th}.	2 days	Clearly defined dry layer between 650-850 mb.

Angström exponent is the name of the exponent in the formula that is usually used to describe the dependency of the aerosol optical depth or extinction coefficient on wavelength.

Depending on particle size distribution, the spectral dependence of the aerosol optical depth is given approximately by

$$\frac{\tau_\lambda}{\tau_{\lambda_0}} = \left(\frac{\lambda}{\lambda_0}\right)^{-\alpha}$$

where τ_λ is the aerosol optical depth or thickness at wavelength λ, and τ_{λ_0} is the aerosol optical depth or thickness at the reference wavelength λ_0. In principle, if the optical depth at one wavelength and the Angström exponent are known, the optical depth can be computed at a different wavelength. In practice, measurements are made of the optical depth of an aerosol layer at two different wavelengths, and the Angström exponent is estimated from these measurements using this formula. The aerosol optical depth can then be derived at all other wavelengths, within the range of validity of this formula.

For measurements of optical depth $\tau_{\lambda_1}$and τ_{λ_2}taken at two different wavelengths $\lambda_1$and λ_2 respectively, the Angström exponent is given by

$$\alpha = -\frac{\log \frac{\tau_{\lambda_1}}{\tau_{\lambda_2}}}{\log \frac{\lambda_1}{\lambda_2}}$$

The Angström exponent is inversely related to the average size of the particles in the aerosol: the smaller the particles, the larger the exponent. Thus, Angström exponent is a useful quantity to assess the particle size of atmospheric aerosols or clouds, and the wavelength dependence of the aerosol/cloud optical properties. For example, cloud droplet, usually with large sizes and thus very smaller Angström exponent (nearly zero), is spectrally neutral, which means, e.g., the optical depth does not change with wavelength.

Figure 6 shows the relationship between the aerosol optical depth and the Angström exponent for the month of July of 2012. Overall, the higher the aerosol optical depth the lower the Angström exponent. A scatter plot such as this, can show the range of variability of the Angström exponent with respect to AOD(500 nm.) This is very useful indeed since the Angström exponent value is related to aerosol particle size. In our graph, Angström values smaller than 0.25 and AOD larger than 0.25 accounts for almost all the dust events (red data points) indicating the presence of dust (larger particles, with larger optical depth).

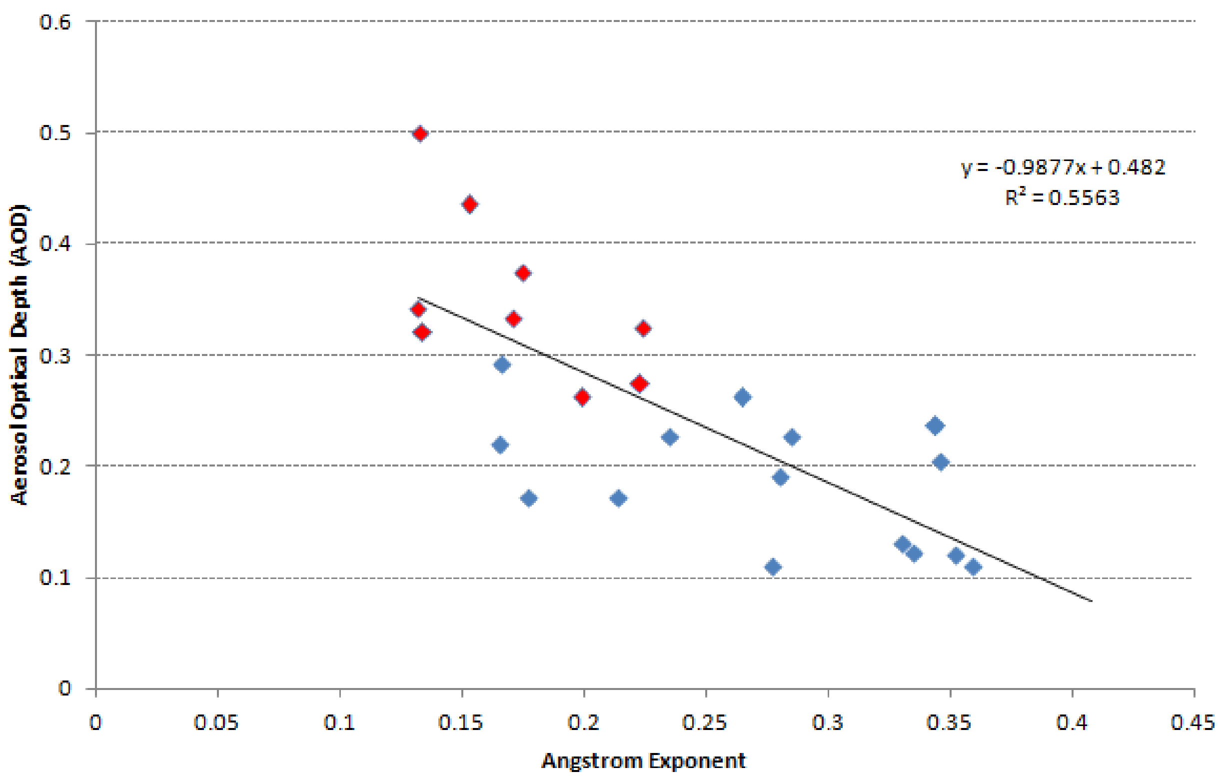

Figure 6. Relationship between the aerosol optical depth and the Anstrom Exponent.

Figure 7 shows the relationship between the aerosol optical depth and the amount of fine particulate matter (PM2.5). The red data points correspond to the Saharan dust events.

This shows that there is an increase in fine particulate matter from a clean background of 20 to 30 micrograms per cubic meter of air (µg/m^3) during the Saharan dust episodes. The average PM2.5 concentration for Saharan dust episodes during the month of July was 69.4 micrograms per cubic meter of air (µg/m^3). For the days with no detectable Saharan dust the average PM2.5 concentration was 34.4 micrograms per cubic meter of air (µg/m^3). The day with the highest AOD (July 25th) corresponds to the highest PM2.5 of 75 micrograms per cubic meter of air (µg/m^3). This suggests that a large portion of the PM2.5 particles measured at the surface are entrained from the free atmosphere. Dust episode 5 from Table 1 shows that the lowest dry layer (900 mb) was observed with this dust episode. Huang et al. (2010) observed in their study that the lowest bound of the Saharan dust occurs at 1-2 km abobe the surface in western Africa and above 0.5 km in the Caribbean sea. With the height of the boundary layer extending on average higher than that a substantial amount of dust will mix in the boundary layer affecting the horizontal visibility.

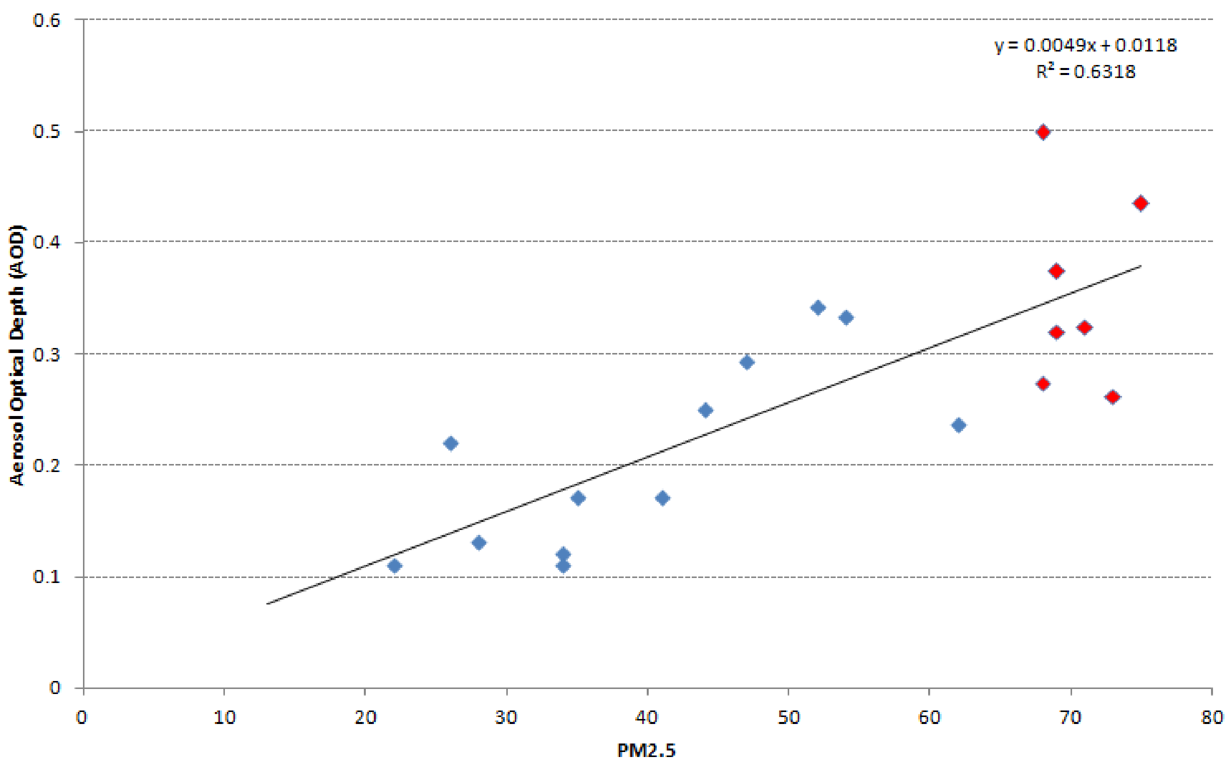

Figure 7. Shows the relationship between the aerosol optical depth and the amount of fine particulate matter (PM2.5)

A comparison was made between the NEMS GFS and NRL NAAPS aerosol models for the six Saharan dust events. Note that the performance was calculated by taking the difference of the forecast AOD (from either model) minus the observed AOD from the AERONET network. A negative number means that the model underestimated the observed AOD by that amount. The results show that overall the models underestimated the observed AOD, with the underestimate of the +60 hr forecast greater than the underestimate of the +12hr forecast. For the Saharan dust events the NEMS GFS and NRL NAAPS are not statistically different for the 12 and 60 hour forecast.

Table 2. Comparison of AOD between the NRL NAAPS and NEMS GFS for each of the Saharan dust events. The last two rows show the averages for all six events as well as the averages for events 1 through 4. The uncertainties in the last two rows are calculated from the standard deviations of each of the six events.

Event	NRL NAAPS +12hr Error	NRL NAAPS +60hr Error	NEMS GFS +12hr Error	NEMS GFS +60hr Error
1	-0.086	-0.236	-0.136	-0.236
2	-0.115	-0.131	-0.131	-0.131
3	-0.102	-0.227	-0.026	-0.102
4	-0.192	-0.242	-0.242	-0.192
5	-0.119	-0.019	-0.089	-0.086
6	-0.034	-0.099	-0.024	-0.024
Average 1-6	-0.108 ± 0.051	-0.159 ± 0.091	-0.108 ± 0.082	-0.128 ± 0.076
Average 1-4	-0.124 ± 0.047	-0.209 ± 0.052	-0.134 ± 0.088	-0.165 ± 0.060

Anectdotal comparison between the forecast images produced by both models suggest that for Saharan dust events with smaller loads of AOD the NRL NAAPS performed better (on regard to timing and geographical coverage), capturing better the gap in Saharan dust between the first two events (Figure 8). Figure 9 shows the forecast of the NEMS GFS model for the same time period. The NEMS GFS does not capture the observed interruption in the Saharan dust observed on the 4th of July. For the last two events of the month, which contained higher AODs the comparison of the NEMS GFS and NRL NAAPS showed similar performance on regard to the timing and geographical coverage of the NEMS GFS and NRL NAAPS.

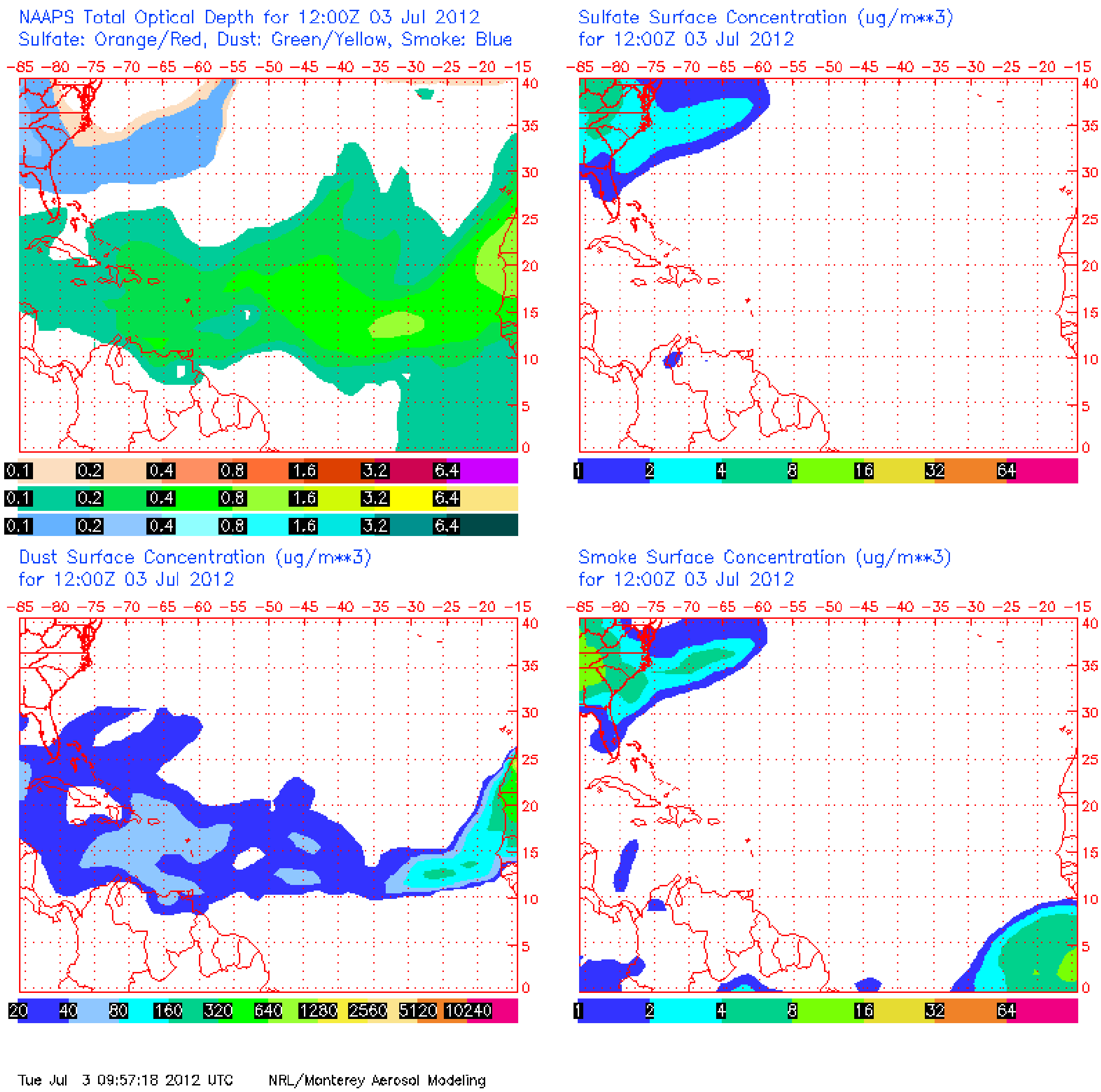

Figure 8. Note the gap in AOD southeast of Florida in this forecast which coincided with the reduction of dust observed on July 4th.

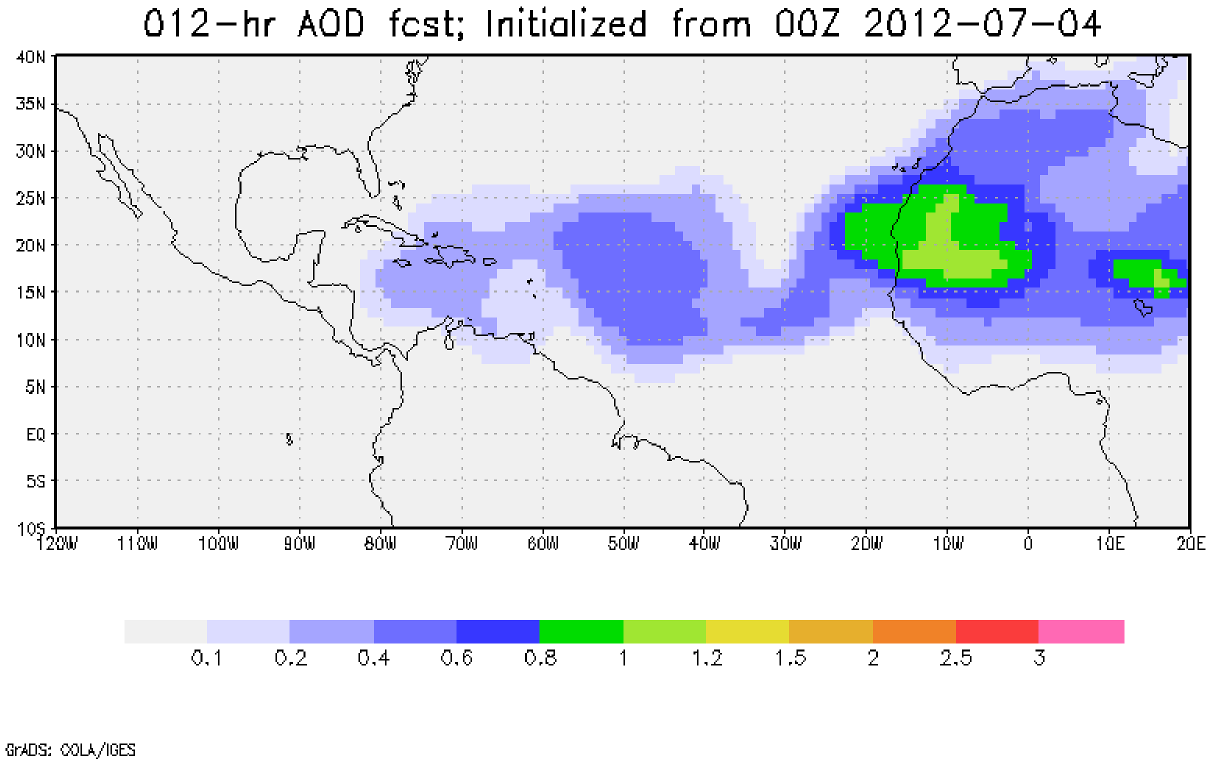

Figure 9. 12-hour forecast of the NEMS GFS for July 4th, 2012.

Each of the 6 Saharan dust episodes were investigated using the Rosenstiel School of Marine & Atmospheric Science, at the University of Miami LIDAR. The arrival of the dust for each episode was observed to occur in a discontinuous manner with patches of dust arriving between the surface and a height of 4 km. Figure 10 shows the arrival of the dust for July 18th (dust episode 3). A more solid aerosol layer is observed on July 19th (dust episode 3) (Figure 11).

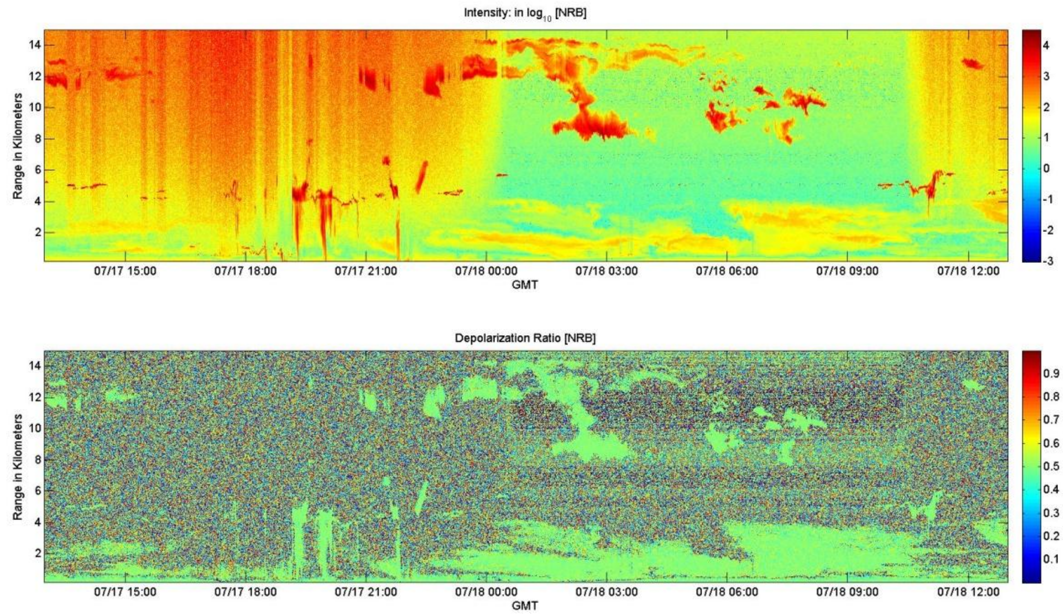

Figure 10. Arrival of the Saharan dust for episode number 3 indicated in Table 1.

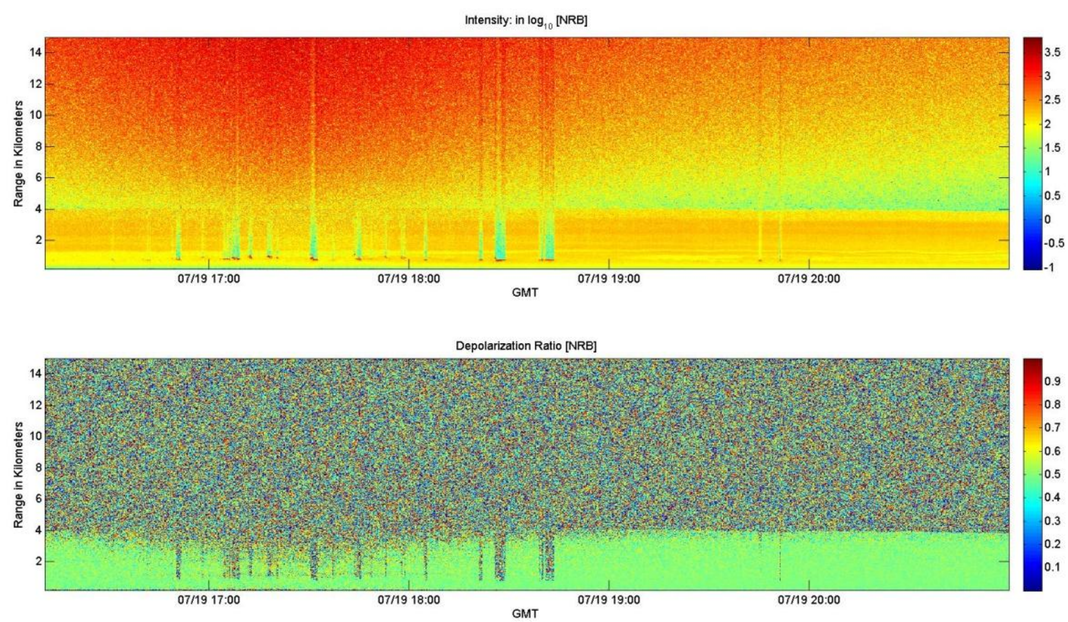

Figure 11. Depiction of the Saharan dust observed on July 19, 2012.

The strong Saharan dust event observed on July 25th shows a stronger return intensity (Figure 12), especially around an altitude of 3 km, than the intensity observed for previous Saharan dust events (e.g. see Figure 11).

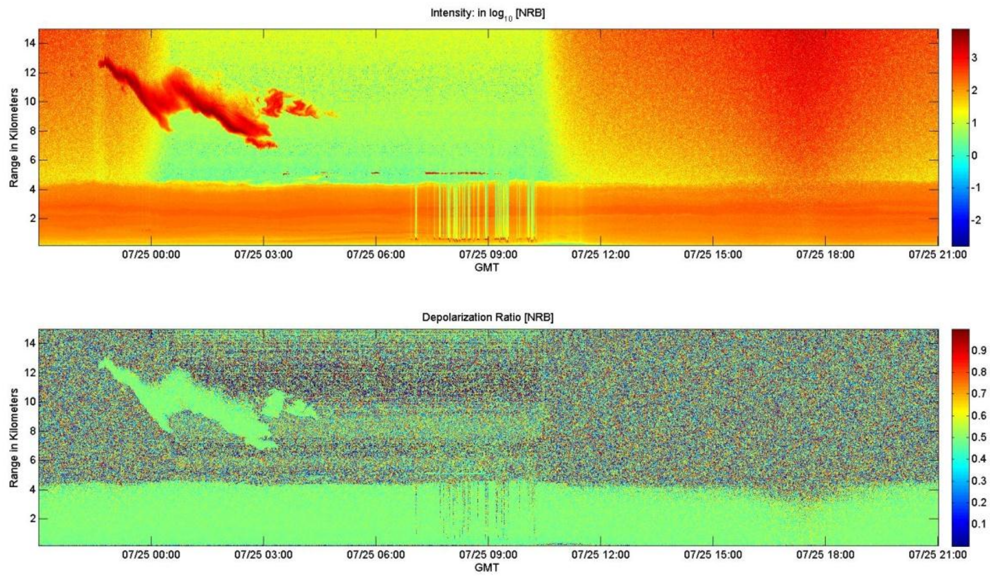

Figure. 12. Strong Lidar signal observed for July 25 (the strongest event of the study).

Figure 13 and 14 show the erosion of the Saharan dust layer for two different events. Event 5 (July 26) showed a gradual decrease in dust due to an air mass change. Figure 13 shows very clearly the presence of stratified layers and vanishing dust above 2 km after 20 UTC on July 26.

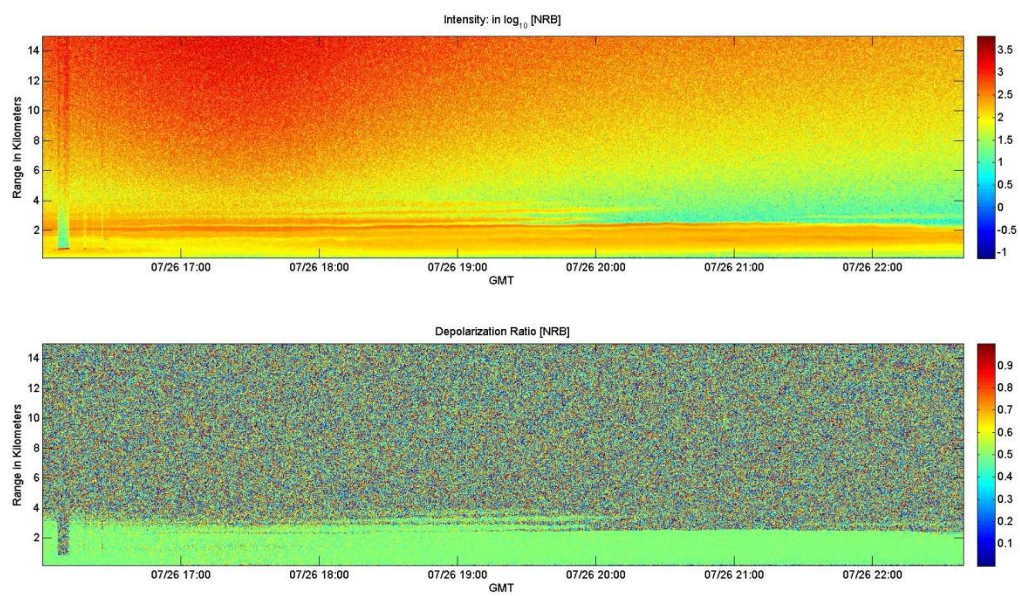

Figure 13. Decrease in Saharan dust observed on July 26, 2012.

Event 3 ended with the intrusion of a few showers moving from the east associated with a change in air mass in the low levels. This was shown clearly in Figure 14 with a decrease in dust in the low levels.

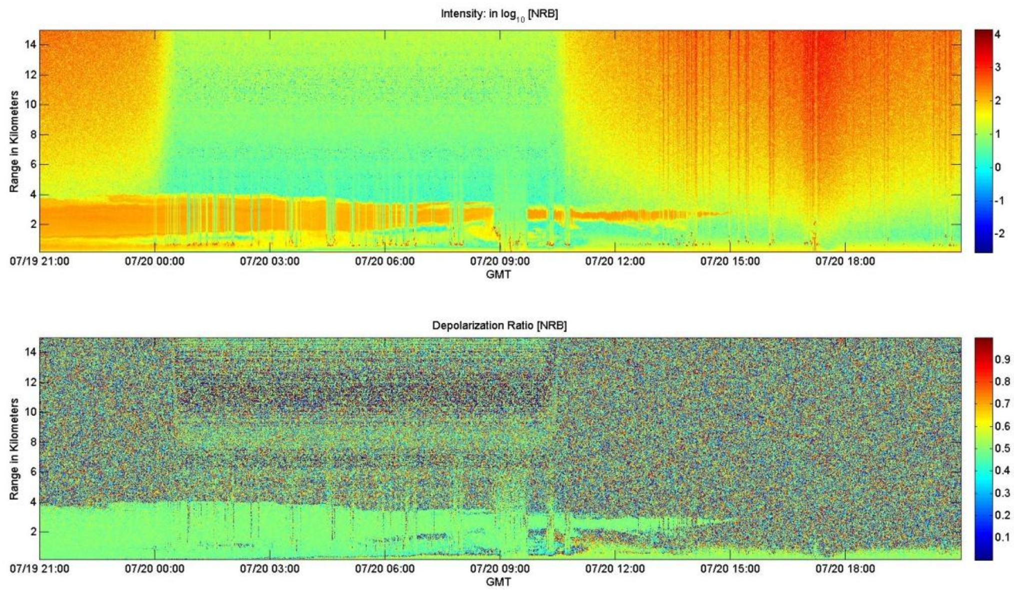

Figure 14. Decrease in Saharan dust starting at the low levels especially after 9 UTC, July 20th.

Figure 15 shows the NASA SPORT TERRA MODIS image for the beginning of dust event 5 (beginning on July 24, 2012). The light purple colors can be seen southeast of Florida beginning to affect the east coast Miami metro areas.

Figure 16 shows the MODIS GOES Hybrid Visible image on July 26, 2012 (2145 UTC) corresponding also to dust episode number 5.

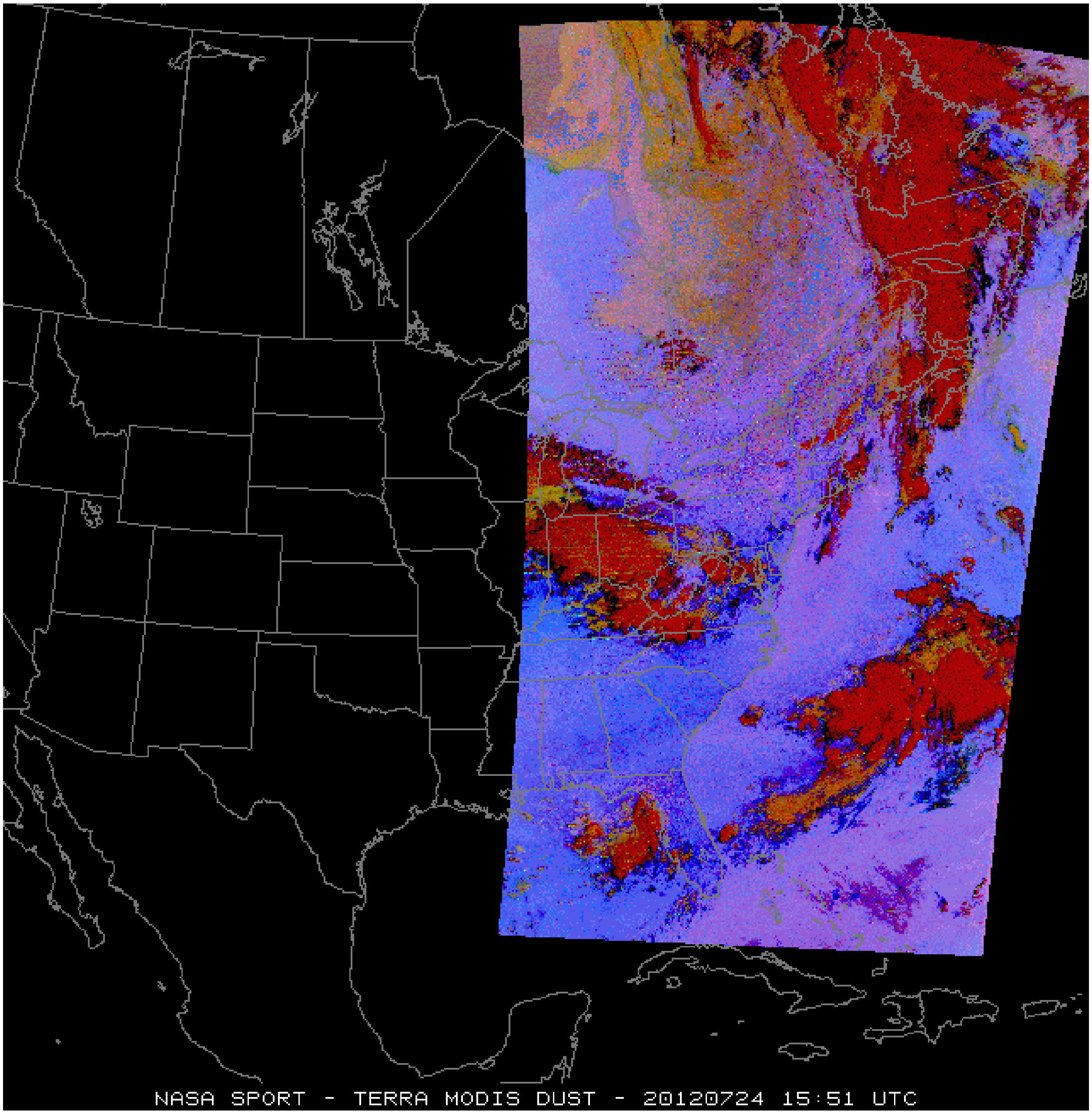

Figure 15. This NASA SPORT TERRA MODIS image shows in light purple colors the dust approaching South Florida from the southeast.

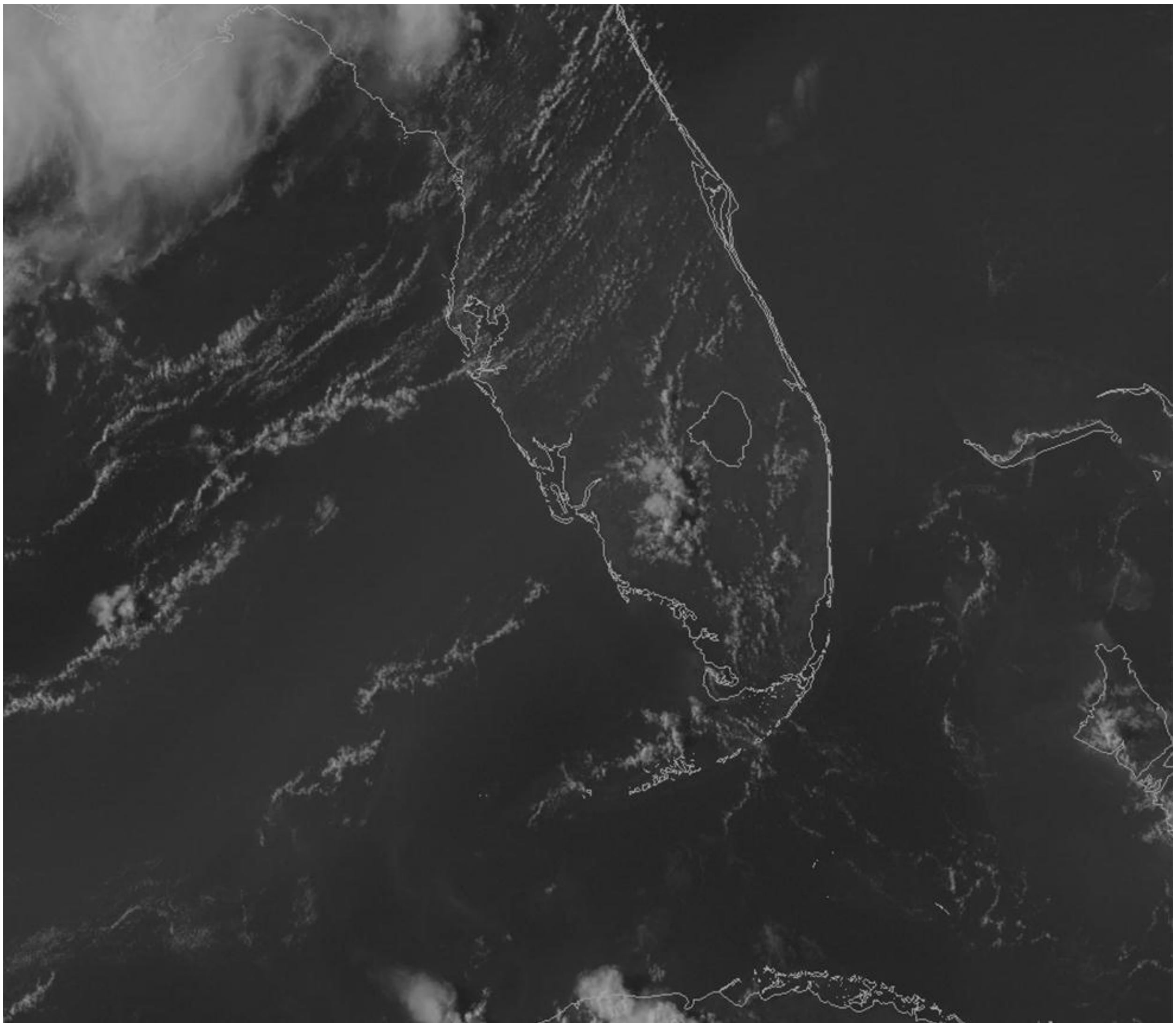

Figure 16. This MODIS GOES Hybrid Visible image taken on July 26, 2012 (2145 UTC) shows the presence of widespread Saharan dust indicated by the dull colors and diminished contrast.

The soundings for the entire month of July were also analyzed to see if the Saharan dust presented itself in conjunction with dry layers anywhere from the surface to 5 km.

4. Conclusions

The amount of Saharan dust was quantified through the use of the aerosol optical depth for 6 Saharan dust events observed at Miami during the month of July of 2012. Surface observations of Aerosol Optical Depth (AOD) from the AERONET (AErosol RObotic NETwork) and a micropulse LIDAR with polarization from the University of Miami South Florida's Cloud-Aerosol-Rain Observatory (CAROb) for several Saharan dust events were observed in Miami

Florida during the month of July of 2012. The surface observations are then compared with aerosol predictions results from the Navy Aerosol Analysis and Prediction System (NAAPS), and the newly appointed GFS model from the National Oceanic and Atmospheric Administration (NOAA) and the National Weather Service (NWS). Details about the vertical extent and evolution of the Saharan dust inside and above the boundary layer were investigated for each event.

The following are the main conclusions:

(1) The average daily AOD for days with Saharan dust was 0.333 with a maximum of 0.499 and a minimum of 0.262. The average daily AOD for days with no noticeable Saharan dust was 0.182 with a minimum of 0.11 and a maximum of 0.293.

(2) Angström values smaller than 0.25 and AOD larger than 0.25 account for almost all the dust events, indicating the presence of dust (larger particles, with larger optical depth).

(3) There is an increase in fine particulate matter from a clean background of 20 to 30 micrograms per cubic meter of air (µg/m^3) during the Saharan dust episodes. The average PM2.5 concentration for Saharan dust episodes during the month of July was 69.4 micrograms per cubic meter of air (µg/m^3). For the days with no detectable Saharan dust the average PM2.5 concentration was 34.4 micrograms per cubic meter of air (µg/m^3).

(4) The results show that for the Saharan dust events the NEMS GFS and NRL NAAPS are not statistically different for the 12 and 60 hour forecast. The results show that overall the models underestimated the observed AOD, with the underestimate of the +60 hr forecast greater than the underestimate of the +12hr forecast.

(5) Anectdotal comparison between the forecast images produced by both models suggest that for Saharan dust events with smaller loads of AOD the NRL NAAPS performed better (on regard to timing and geographical coverage) capturing better the gap in Saharan dust between the first two events. The NEMS GFS does not capture the observed interruption in the Saharan dust observed on the 4th of July. For the last two events of the month, which contained higher AODs the comparison of the NEMS GFS and NRL NAAPS showed similar performance on regard to the timing and geographical coverage of the NEMS GFS and NRL NAAPS.

(6) The use of the LIDAR with polarization from the University of Miami South Florida's Cloud-Aerosol-Rain Observatory (CAROb) was key to show the vertical characteristics of

the Saharan dust. The Saharan dust extended from the surface to 4 km. The most intense event was observed between July 24 and 25th, showing dust up to 4.5 km with the densest layer between 2.5 to 3 km. The evolution of a few dust events were shown in this paper.

REFERENCES

Goddard Space Flight Center, cited 2012: AERONET: Aerosol Robotic Network. [Available online at http://aeronet.gsfc.nasa.gov/]

Goddard Space Flight Center, cited 2012: Saharan Dust Affects Thunderstorm Behavior in Florida. [Available online at http://www.nasa.gov/vision/earth/lookingatearth/florida_dust.html]

Naval Research Laboratory, cited 2012: Monterey Aerosol Page. [Available online at http://www.nrlmry.navy.mil/aerosol_web/]

Rosenstiel School of Marine and Atmospheric Science/Kenneth Voss, cited 2012: CAROb micropulse lidar. [Available online at http://carob.rsmas.miami.edu/mpl.html]

Lau, K. M. and K. M. Kim, 2007: Cooling of the Atlantic by Saharan dust. *Geophys. Res. Lett*., doi:10.1029/2007/GL031538.

Zhao C, X Liu, LR Leung, and S Hagos, 2011: Radiative impact of mineral dust on monsoon precipitation variability over West Africa. *Atmospheric Chemistry and Physics* 11(5):1879-1893, DOI: 10.5194/acp-11-1879-2011.

Susan C. van den Heever, Gustavo G. Carrio, William R. Cotton, Paul. J. DeMott and Anthony J. Prenni, 2009: Saharan dust particles nucleate droplets in eastern Atlantic clouds, *Geophys. Res. Lett*., vol. 36, L01807, 6 PP, doi:10.1029/2008GL035846.

Jingfeng Huang, Chidong Zhang, Joseph M. Prospero, African dust outbreaks, 2010: A satellite perspective of temporal and spatial variability over the tropical Atlantic Ocean, *J. Geohys. Res*,vol. 115, D05202, 20 PP, doi:10.1029/2009JD012516.